REPORTS@SCM

AN ELECTRONIC JOURNAL OF THE
SOCIETAT CATALANA DE MATEMÀTIQUES

A Finite Element Method solution to the Phase-Field model of the Stefan problem

*Max Orteu
Freie Universität Berlin
maxorteu@zedat.fu-berlin.de

Esther Sala-Lardies
Universitat Politècnica de Catalunya
esther.sala-lardies@upc.edu

Sonia Fernàndez-Méndez
Universitat Politècnica de Catalunya
sonia.fernandez@upc.edu

∗Corresponding author

Resum *(CAT)*
Aquest treball es centra en el model de camp de fase per al problema d'Stefan, així com en la solució numèrica amb el mètode dels elements finits per a simular exemples en dues dimensions.

Abstract *(ENG)*
This work is concerned with the Phase-Field model of the Stefan problem, as well as the numerical solution with the Finite Element Method to simulate examples in two dimensions.

Keywords: *heat diffusion, numerical methods, PDEs, modeling, FEM, Phase-Field models, Stefan, solidification.*
MSC (2010): *65N30, 80A22, 80M10.*
Received: *July 28, 2022.*
Accepted: *September 29, 2022.*

Acknowledgement
This work was supported by Generalitat de Catalunya (2017-SGR-1278).

1. Introduction

The Stefan problem, first introduced by Josef Stefan in [12] in the context of polar ice caps, is a boundary value problem used to model the state of systems where phase transitions occur. It is a free boundary problem; that is, a partial differential equation (PDE) to be solved for an unknown domain, or in a domain with unknown interface. In this work, biphasic systems modeling a Liquid-Solid coexistence, and featuring a pure substance are considered. A solution to the problem should be able to describe the position of the moving interface $\gamma(t)$ between the two different states of the given material, as well as the temperature at each point in the space-time domain, $u(x, t)$; all this, depending on a given a set of initial and boundary conditions. A classical example could be the melting of an ice cube in a glass of water, where the equations should provide the distribution of ice for any given time t, and the temperature at each point in space and time.

The model we have chosen to approximate solutions to the Stefan problem is the so-called Phase-Field model (PF). Phase-Field models are widely used in transformation problems, since they facilitate the tracking of the interface. The main idea is to consider what is called the Phase-Field function or order parameter (in this work noted as ϕ), a scalar function that equals a fixed constant in each phase and varies rapidly, but smoothly (in our case from -1 to $+1$), in the interface region. The phase transformation occurs inside a finite-width region, whose thickness is a parameter in the model, here noted as ξ, and where in general the transport properties are assumed to vary with u. It is worth mentioning that the solution tends to a Sharp-Interface model as $\xi \to 0$. An important resource for the study of this modeling technique has been [11].

When it comes to the numerical method used to obtain the solutions, the Finite Element Method (FEM) has been chosen. It is a powerful and popular method, used in areas such as solid mechanics [9], electromagnetic potentials [10], or heat transfer – as it is here the case. One of its most salient advantages is that it allows modeling complex and irregular geometries, given that it is capable of working under non-uniform meshes. This is important because it makes it possible to capture local effects by calculating the solution on a partially-refined domain, a process which helps produce accurate yet not so computationally-demanding solutions.

This work serves as a stepping stone to implementing an adaptive solution to the Phase-Field model of the Stefan problem. Such a procedure, inspired by the work of Alba Muixí in the context of crack propagation in [9], would constitute an efficient solution that would drastically decrease the running time involved and capture much better the local phenomena. This would in turn make it possible to calculate approximations with finer meshes (and subsequently smaller time steps), allowing for $\xi \to 0$, conditions under which, as mentioned, the Phase-Field model converges to the Sharp-Interface model.

2. The Phase-Field model for the Stefan problem

The classical Stefan problem arises when we consider two phases of a material undergoing a phase transformation. A heat equation must be solved for each phase, but with the added difficulty of having a boundary on a moving interface, where the temperature is fixed. That is why we say that we have a free boundary

problem. A further equation, the Stefan condition (1c), is needed in order to have a mathematically closed system. With this, the general form of the equations of the Stefan problem for a domain Ω are

$$\frac{\partial u}{\partial t} = \nabla \cdot (c_l \nabla u), \quad x \in \Omega_l(t), \tag{1a}$$

$$\frac{\partial u}{\partial t} = \nabla \cdot (c_s \nabla u), \quad x \in \Omega_s(t), \tag{1b}$$

$$lv = c_s \frac{\partial u}{\partial n}\Big|_{x \downarrow \gamma(t)} - c_l \frac{\partial u}{\partial n}\Big|_{x \uparrow \gamma(t)}. \tag{1c}$$

Here u is the temperature and the domain is divided into Ω_l and Ω_s, where the material is in liquid and solid phase, respectively. For each of these subdomains, c_l and c_s are the diffusivity constants of the material. Lastly, l is the latent heat per unit volume, while $\gamma(t)$ is the position of the interface and v its normal velocity.

Equations (1) are referred to here as Sharp-Interface model. The main difficulty of the FEM for solving them comes from the fact that the computational mesh must be fitted to the interface $\gamma(t)$ to represent the weak discontinuity of the temperature. This requires a continuous mesh adaptation that is cumbersome and computationally expensive.

To circumvent this, Phase-Field models consider a smooth variation of the temperature across the interface. To do so, a Phase-Field variable ϕ is introduced, taking the value $+1$ in the liquid domain, -1 in the solid, and varying smoothly between these values in a thin transition region, with the value 0 at the interface.

2.1 Phase-Field models

The derivation of mathematical Phase-Field models from physical principles is built upon Landau–Ginzburg theory of phase transitions, which can be found in [7]. The Phase-Field model presented here is based on the work by Cahn and Hilliard in [3] and features the variables u and ϕ, which account for the temperature and the phase state at each point in the space-time domain. There are several Phase-Field models for the Stefan problem in the literature, most notably the ones based on the Kobayashi and the Caginalp potentials. For the Kobayashi potential, originally introduced in [6], we have followed Fabbri and Voller, but with a change of sign to fix the typo in equation (2.7) in [5]. An important reference for this section has been [8], where a thorough explanation of the Phase-Field model for the Stefan problem can be found.

Given a domain Ω and its boundary $\Gamma = \partial\Omega$, the Phase-Field model for the Stefan problem is a coupled system of two PDEs. If we consider the system in a time interval $[0, T]$, these are:

$$\begin{cases} \dfrac{\partial u}{\partial t} = c\Delta u - \dfrac{l}{2}\dfrac{\partial \phi}{\partial t} & \text{in } \Omega \times [0, T], \quad (2a) \\ \alpha\xi^2 \dfrac{\partial \phi}{\partial t} = \xi^2 \Delta \phi - \dfrac{\partial F}{\partial \phi} & \text{in } \Omega \times [0, T], \quad (2b) \end{cases}$$

with initial conditions $u(x, 0) = u_0(x)$, $\phi(x, 0) = \phi_0(x)$ and boundary conditions.

Equation (2a) is a heat equation, modified by the Phase-Field term. Here, $u(x, t)$ represents $T(x, t) - T_M$, where $T(x, t)$ is the temperature of the material and T_M the temperature at which the change of

phase takes place – in Liquid-Solid equilibrium, the fusion/solidifying temperature. In practice, we can think of solidification/fusion in an ice-water system, where $T_M = 0$, and so $T(x,t) = u(x,t)$. An important part of the model is the recovering potential F appearing in (2b), which is a double-well potential that has its minima at the values of ϕ corresponding to the two different phases. The two recovering potentials previously mentioned are

$$\text{Caginalp: } F(u,\phi) = \frac{1}{8a}(\phi^2-1)^2 - \frac{\Delta s}{2}\phi u, \tag{3}$$

$$\text{Kobayashi: } F(u,\phi) = \frac{W}{16}\int_0^{\phi}(r^2-1)(r+2b(u))\,dr, \tag{4}$$

where a is a parameter exclusive of the Caginalp potential that should be chosen so that $\frac{\partial F}{\partial \phi}$ has minima near 0, -1 and $+1$, W is a constant with units of energy per unit volume, and Δs is the entropy scale, defined as the difference between the entropies of the liquid and solid phases at the melting temperature.

From a theoretical standpoint, both expressions (3) and (4) result in a double-well potential, with minima at ± 1 when taking sufficiently small values of u, and considering $F(u,\phi)$ as a function of ϕ. However, while for the Kobayashi potential these minima are fixed, in the Caginalp potential they shift from ± 1 as u moves away from 0 (see Figure 1). This effect fades away as $\xi \to 0$ and $a \to 0$, nonetheless, this potential in practice produces values of $|\phi| > 1$, which hinders the interpretation of the results. Consequently, we employ the Kobayashi potential for practical examples.

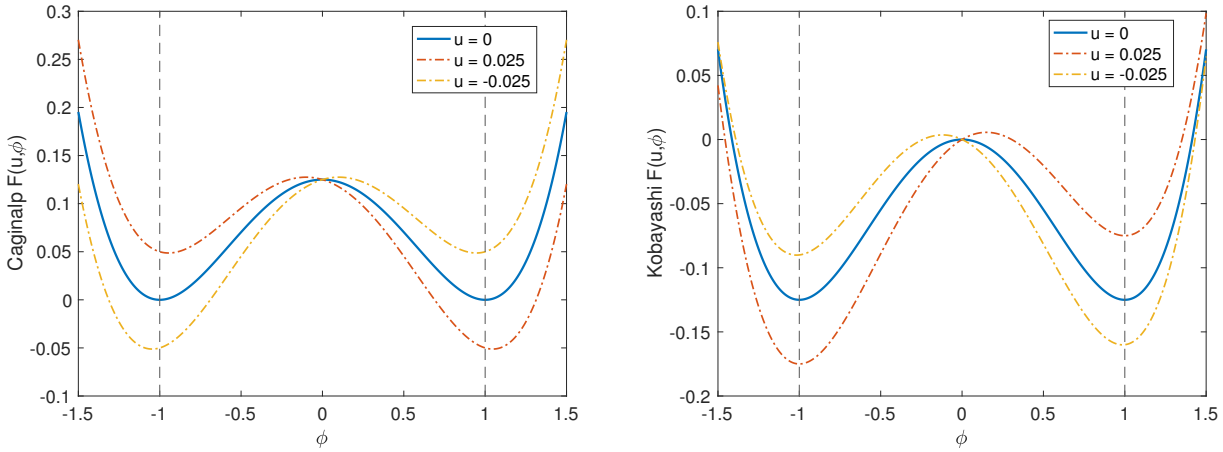

Figure 1: Caginalp (left) and Kobayashi (right) potentials as functions of ϕ, for three different values of u $(-0.025, 0, 0.025)$. In the first case, the minima depart from ± 1 as u drifts away from 0, while in the second they remain in the same place. The parameters of the models are taken as mentioned in Subsection 2.2, $a = 1$, $W = 8$, $\Delta s = 4$.

The reader should note that c has been taken in (2a) as constant and equal in both phases, as will be the case in the whole of this work. Regarding the new parameters in the Phase-Field model, in (2b) α is a timescale parameter and ξ is the Phase-Field energy parameter or gradient-energy coefficient, and it controls the interface width. Sometimes the notation $\tau = \alpha\xi^2$ is used, with τ being the time relaxation parameter. A detailed outline of parameters can be found in the work by Caginalp in [2].

2.2 Interpretation of the model and assumptions

The dynamical interpretation for equations (2a) and (2b) is as follows. Equation (2a) is a Fourier heat equation in which a source term has been added to factor in the latent heat release at the moving interface. On the other hand, the phase equation (2b) is a linear time evolution that features the imbalance between the excess interface free-energy and the restoring potential $F(u, \phi)$.

Throughout the examples, we have considered a constant diffusivity coefficient $c = 1$ and a latent heat $l = 1$. Although these coefficients usually vary between phases and with temperature, respectively, this approximation is valid to study the behavior of the equations. Indeed, this same assumption is found in an important part of the literature (see, for instance, [2] and [8]). Also, in all cases we have considered a pure substance, so that no gradients of concentration appear in the equations and only one set of material parameters is needed.

Regarding the parameters of the Phase-Field model with the Kobayashi potential, we have used $\alpha = 1$, $W = 8$, $\Delta s = 4$, and following Wheeler et al. in [14], $b(u)$ (which should be a monotonic increasing function of$u$ satisfying $|b(u)| < 1/2$) is taken as $b(u) = 6u\Delta s/W$.

Taking into account all of the above, the system of equations (2) with the Kobayashi potential can be re-written as:

$$\begin{cases} \dfrac{\partial u}{\partial t} = c\Delta u - \dfrac{l}{2}\dfrac{\partial \phi}{\partial t} & \text{in } \Omega \times [0, T], \\ \alpha\xi^2 \dfrac{\partial \phi}{\partial t} = \xi^2 \Delta\phi + G(u, \phi) & \text{in } \Omega \times [0, T], \end{cases} \tag{5}$$

with $G(u, \phi) = \frac{1}{16}W\phi + \frac{3}{4}u\Delta s - \frac{1}{16}W\phi^3 - \frac{3}{4}u\phi^2\Delta s$.

One final comment to be made is that, in most cases, we have considered homogeneous Neumann boundary conditions for both u and ϕ, simulating an isolated system. An important caveat is that, when doing so, one has to be careful that the interface (i.e. $\{x \in \Omega : \phi(x, t) = 0\}$) remains far away enough from the boundary with Neumann conditions, since the interface is by definition a region with strong gradients in the Phase-Field variable ϕ, and both conditions cannot coexist.

3. Examples

3.1 2D analog of a known 1D Stefan problem

The goal of this first example is to validate the Phase-Field model and its numerical solution. To this end, we consider the work by Surana et al. in [13], which features a 1D Stefan problem (with sharp interface) with a known analytical solution.

$$u_a(x, t) = \begin{cases} C_1 \dfrac{\operatorname{erf}\left(\frac{\beta}{2}\right) - \operatorname{erf}\left(\frac{x}{2\sqrt{t+t_0}}\right)}{\operatorname{erf}\left(\frac{\beta}{2}\right)}; & x \le \gamma(0), \\ C_2 \dfrac{\operatorname{erf}\left(\frac{\beta}{2}\right) - \operatorname{erf}\left(\frac{x}{2\sqrt{t+t_0}}\right)}{\operatorname{erfc}\left(\frac{\beta}{2}\right)}; & x > \gamma(0), \end{cases}$$

$$\gamma(t) = \beta\sqrt{t + t_0}.$$

The problem is stated in $\Omega = [0, 1]$ with constant Dirichlet boundary conditions at $x = 0$: $u(0, t) = u_a(0, t)$. The initial condition for the PF function $\phi(x, 0)$ is calculated here as the stationary solution to equation (5) neglecting the laplacian term, i.e., $G(u(x, 0), \phi(x, 0)) = 0$. At $x = 1$, homogeneous Neumann boundary conditions are imposed for u.

In our case, we consider a rectangular domain $\Omega = [0, 1] \times [0, 0.04]$, and use a 2D analog of the boundary and initial conditions employed by Surana et al., treating them as functions of x and independent of the y-variable.

Indeed, for the boundary conditions, we use $u(0, y, t) = u_a(0, t)$, and calculate $\phi(0, y, t)$ such that $G(u, \phi) = 0$. For the rest of the boundary, homogeneous Neumann boundary conditions are employed for both u and ϕ.

As in [13], the parameters are chosen as $C_1 = -0.085$, $C_2 = -0.015$, $t_0 = 0.1246$, $\beta = 0.396618$. This translates into $\gamma(0) = 0.14$ and we can see that at this point the initial condition has a discontinuity in the derivative of the temperature. It can also be observed in Figures 2 and 3 that the 0-level set of ϕ is a good approximation to the position of the interface.

With respect to the numerical parameters of the models, $m = 150$ space intervals have been used, which makes an element size $h = 0.0067$. The limit $\xi \geq 1.25h$ as proposed by Fabbri and Voller in [5] when using fixed-grid methods is employed and, consequently, $\xi = 0.0083$ has been chosen, to have the minimum possible ξ without instability in the solution. In this case, we choose a final time of $T = 0.5$.

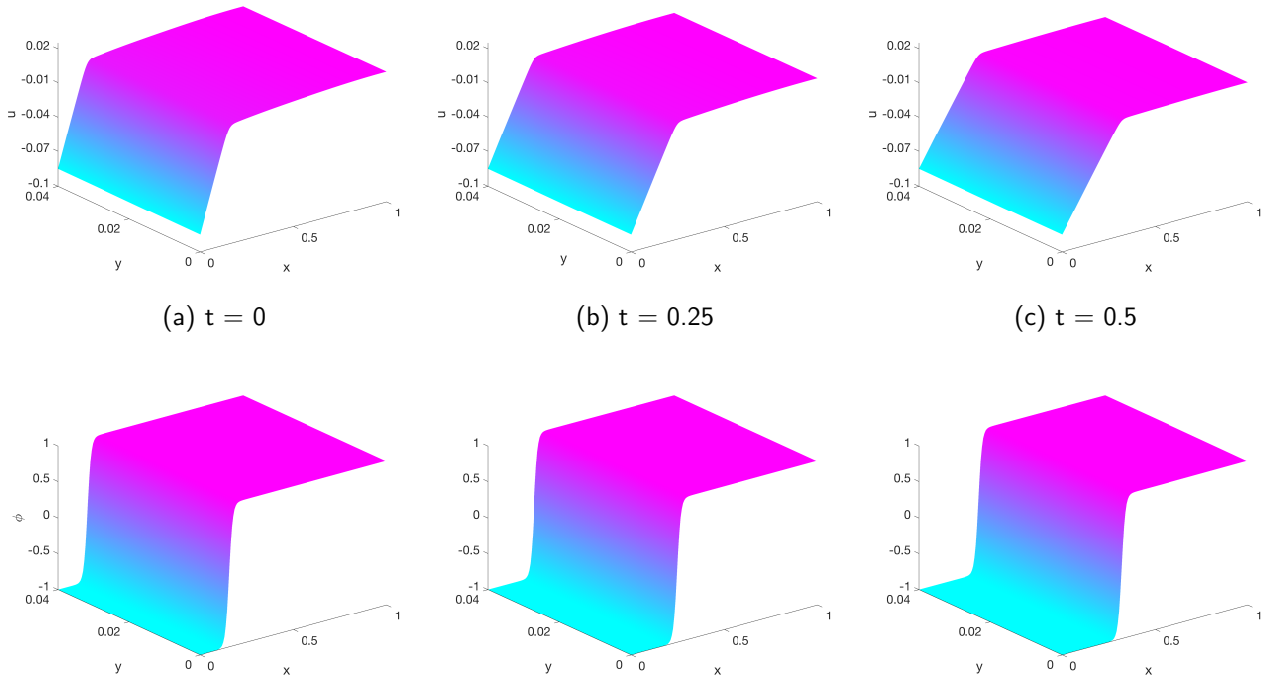

(a) t = 0 (b) t = 0.25 (c) t = 0.5

(d) t = 0 (e) t = 0.25 (f) t = 0.5

Figure 2: Temperature $u(x, y, t)$ (above) and PF $\phi(x, y, t)$ (below) obtained with the Kobayashi computational model of the 2D analog of the problem considered in Subsection 3.1.

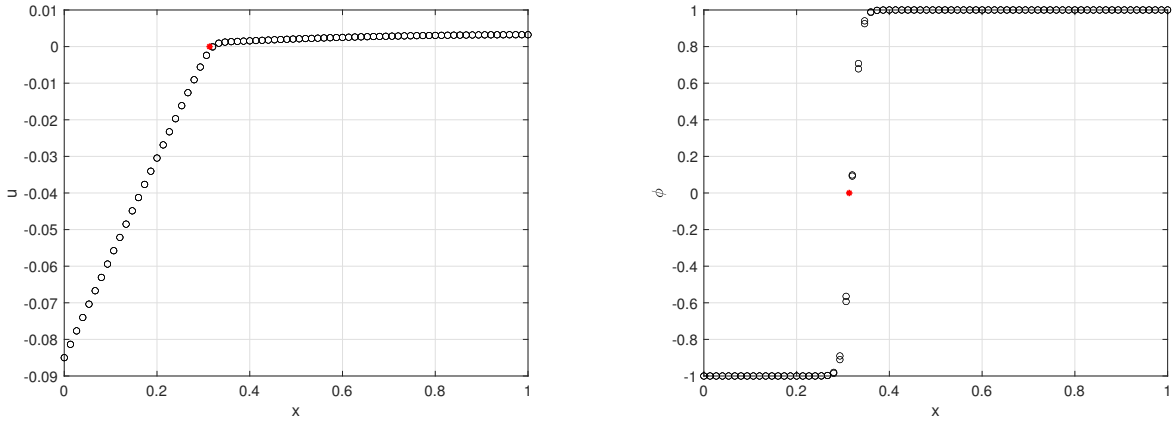

Figure 3: Temperature u (left) and PF ϕ (right) as a function of x for $t=0.5$. In each case, a red star shows the analytical position of the interface, whose behavior is successfully replicated by the calculated solution.

3.2 Freezing with circular symmetry

In this section, we use the 2D FEM code to calculate a solution to the Stefan problem in a square domain with a circular hole, i.e., $\Omega = (0,1)^2 \backslash B((0.5,0.5),0.05)$. The interest of this example, apart from its physical meaning, is that it motivates the need for an unstructured mesh. In addition to this, for the first time, a partial refinement of the domain is used (see Figure 4). This is, only the elements in which a phase transformation can occur are refined.

We first start with Dirichlet boundary conditions on the boundary of the circle, $u = -0.015$, while we use homogeneous Neumann conditions on the outer rectangle, simulating an isolated system. Regarding the initial condition, we use

$$u(x,y,0) = \begin{cases} -0.015, & \text{if } (x-0.5)^2 + (y-0.5)^2 \leq 0.075^2, \\ 0.015, & \text{otherwise,} \end{cases}$$

and again calculate ϕ from the value of u. Figure 5 shows the results obtained in the simulation using the model parameters $\alpha = 1$ and $\xi = 0.0075$, element size $h = 0.006$, and final time $T = 0.025$.

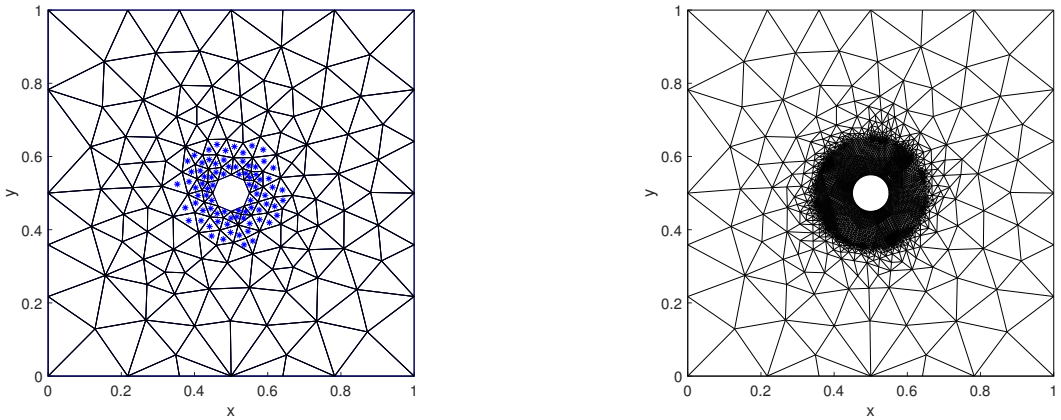

Figure 4: The initial mesh (left) is refined repeatedly until all elements close to the initial interface are small enough to capture a subsequent phase transition. The right image shows the final mesh used in the calculations.

If we take a close look as in the left of Figure 6, where the values of u are plotted as a function of the radius to the center of the domain, we can see that there is now no spike in the temperature. This is thanks to the smoothing effect of the laplacian term. Finally, on the right of Figure 6, there is a contour plot of the points of the domain for which $u = 0$ at four different moments in time. As expected from a physical point of view, this shows a circle that expands with time but maintains its shape, a direct consequence of the circular symmetry of the example. We can conclude that the Phase-Field model excels at tracking the evolution of an existing interface.

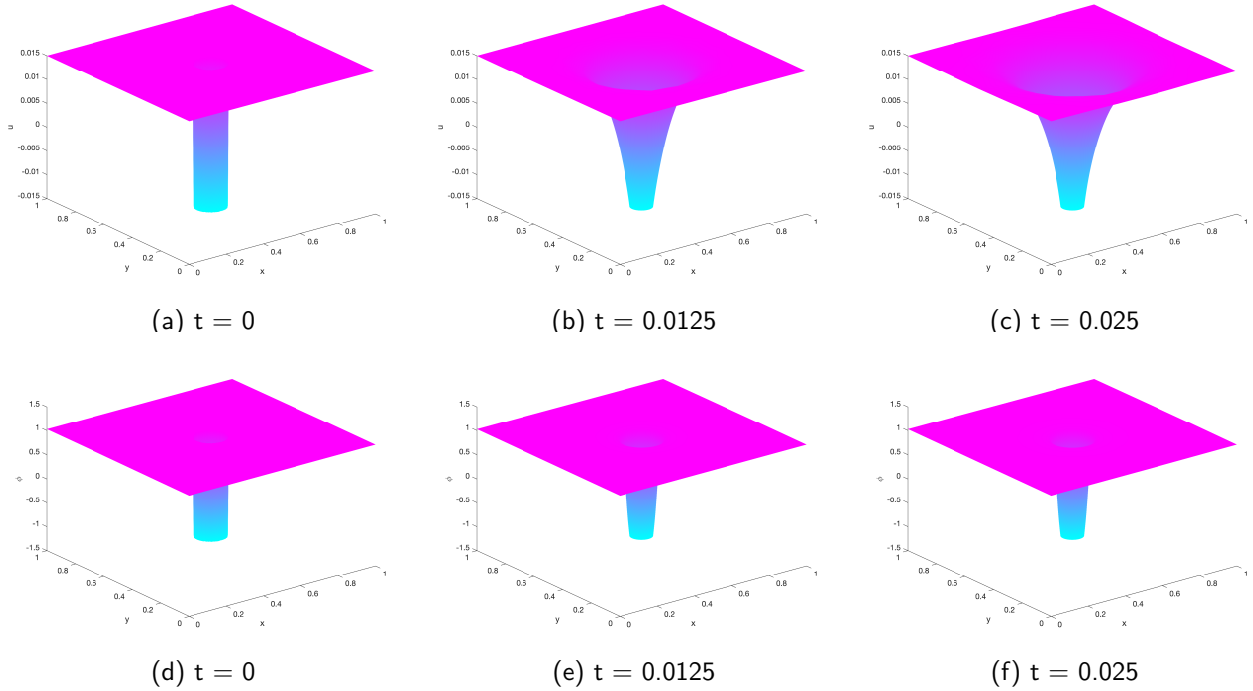

(a) t = 0 (b) t = 0.0125 (c) t = 0.025

(d) t = 0 (e) t = 0.0125 (f) t = 0.025

Figure 5: FEM solution for $u(x, t)$ (above) and $\phi(x, t)$ (below) for a domain with one hole and initial interface. The following numerical parameters are used: $h = 0.006$, $\xi = 0.0075$, $T = 0.025$, $\Delta t = 6.21e - 08$.

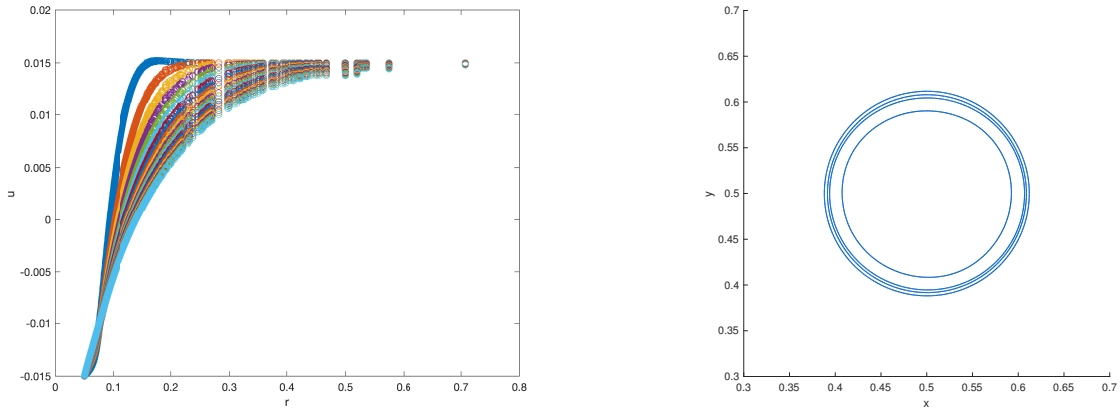

Figure 6: Behavior of the solution when an initial interface is provided. On the left, temperature is represented as a function of the radius, for twenty evenly spaced instants. On the right, the projected view of the level curves for which $u = 0$ is shown at times $t_0 = 0$, $t_1 = 0.008$, $t_2 = 0.017$ and $t_3 = 0.025$.

4. Numerical solution

4.1 Weak form and discretization

We start from the system of equations (2) of the Phase-Field model for the Stefan problem in a general domain Ω, with given Dirichlet boundary conditions $u(\Gamma_u) = u_D$ and $\phi(\Gamma_\phi) = \phi_D$, and homogeneous Neumann boundary conditions $\partial u/\partial n(\partial\Omega\backslash\Gamma_u) = 0$ and $\partial\phi/\partial n(\partial\Omega\backslash\Gamma_\phi) = 0$.

To solve this system of PDEs using the Finite Element Method, we must first write the weak form of the problem. First, we multiply both sides by test functions v, w such that $v(x) = 0$ on Γ_u and $w(x) = 0$ on Γ_ϕ, we integrate by parts the terms that contain a laplacian operator and impose the homogeneous Neumann boundary conditions to obtain:

$$\begin{cases} \displaystyle\int_\Omega v\frac{\partial u}{\partial t} = -c\int_\Omega \nabla v\cdot\nabla u - \frac{l}{2}\int_\Omega v\frac{\partial\phi}{\partial t}, \\ \displaystyle\alpha\xi^2\int_\Omega w\frac{\partial\phi}{\partial t} = -\xi^2\int_\Omega \nabla w\cdot\nabla\phi + \int_\Omega wG(u,\phi). \end{cases} \tag{6}$$

Now, the problem consists on finding $u(x,t), \phi(x,t) \in H^1(\Omega)$ such that $u(x,t) = u_D$ on Γ_u, $\phi(x,t) = \phi_D$ on Γ_ϕ and so that (6) is satisfied for all $v, w \in H^1(\Omega)$ such that $v = 0$ on Γ_u and $w = 0$ on Γ_ϕ.

We discretize (6) with a piece-wise polynomial base and approximate $u(x,t)$ and $\phi(x,t)$ as follows:

$$u(x,t) \simeq u^h(x,t) = \sum_{i=1}^{n} u_i(t)N_i(x), \quad \phi(x,t) \simeq \phi^h(x,t) = \sum_{i=1}^{n}\phi_i(t)N_i(x).$$

We denote by $\mathcal{B}_u$, $\mathcal{B}_\phi$ the set of indexes of all nodes on the Dirichlet boundaries Γ_u and Γ_ϕ respectively, for which we already know the values u_i and ϕ_i. Substituting into the weak form $v = N_i$ (for $i \notin \mathcal{B}_u$) and $w = N_i$ (for $i \notin \mathcal{B}_\phi$), and $u(x,t) \simeq u^h(x,t)$, $\phi(x,t) \simeq \phi^h(x,t)$ we obtain the following system of equations

$$\begin{cases} \displaystyle\sum_{j=1}^{n}\int_\Omega N_iN_j\frac{\partial u_j}{\partial t} = -c\sum_{j=1}^{n}\int_\Omega \nabla N_i\cdot\nabla N_j u_j - \frac{l}{2}\sum_{j=1}^{n}\int_\Omega N_iN_j\frac{\partial\phi_j}{\partial t}, & i \notin \mathcal{B}_u, \\ \displaystyle\alpha\xi^2\sum_{j=1}^{n}\int_\Omega N_iN_j\frac{\partial\phi_j}{\partial t} = -\xi^2\sum_{j=1}^{n}\int_\Omega \nabla N_i\cdot\nabla N_j\phi_j + \sum_{j=1}^{n}\int_\Omega N_iN_jG(u_j,\phi_j), & i \notin \mathcal{B}_\phi, \end{cases}$$

where instead of computing the integral $\int_\Omega N_jG(u,\phi)$, which would be computationally costly, the approximation $G(u,\phi) \approx \sum_j G(u_j,\phi_j)N_j$ is used. This introduces the same error as a spline interpolation, which approximates the calculation with an error h^{p+1}, with p being the order of the polynomial employed. Given that in all cases, we use linear basis functions, which translates into an h^2 error. This coincides with the error due to the FEM method, and so the convergence remains unaffected.

If we use

$$M_{ij} = \int_\Omega N_iN_j\,d\Omega, \quad K_{ij} = \int_\Omega \nabla N_i\cdot\nabla N_j\,d\Omega, \quad i \notin \mathcal{B}, \quad j = 1,\dots,n.$$

We can rewrite the whole system as

$$\begin{cases} M\dot{u} = -cKu - \frac{l}{2}M\dot{\phi}, \\ \alpha\xi^2 M\dot{\phi} = -\xi^2 K\phi + MG(u,\phi), \end{cases}$$

where $G(u,\phi)$ denotes the vector with components $G(u_i,\phi_i)$.

At the time of implementation, we divide the vectors u, ϕ and matrix M in their components on the Dirichlet boundary and in the rest of the domain. Noting them by the subscripts $_F$ and $_I$, respectively, we can write:

$$M = \left[\begin{array}{c|c} M_{II} & M_{IF} \end{array}\right], \quad u = \begin{bmatrix} u_I \\ u_F \end{bmatrix}, \quad \phi = \begin{bmatrix} \phi_I \\ \phi_F \end{bmatrix}.$$

With this decomposition, the system can be written as

$$\begin{cases} M_{II}\dot{u}_I = -M_{IF}\dot{u}_F - cKu - \dfrac{l}{2}M\dot{\phi}, \\ \alpha\xi^2 M_{II}\dot{\phi}_I = -\alpha\xi^2 M_{IF}\dot{\phi}_F - \xi^2 K\phi + MG(u,\phi). \end{cases} \tag{7}$$

We solve (7) at each time step using Euler's method (an explicit, 1st order method):

$$u_I^{n+1} = u_I^n + \Delta t M_{II}^{l,-1}\left(-M_{IF}\dot{u}_F - cKu - \frac{l}{2}M\dot{\phi}\right), \tag{8a}$$

$$\phi_I^{n+1} = \phi_I^n + \frac{\Delta t}{\alpha\xi^2} M_{II}^{l,-1}(-\alpha\xi^2 M_{IF}\dot{\phi}_F - \xi^2 K\phi + MG(u,\phi)). \tag{8b}$$

This is the final system that can be found in the code. For each time step, for efficiency purposes, $\dot{\phi}$ is first computed and used in (8a) and (8b). The reader should note the l superindex in the matrix M, which indicates that we use the lumped mass matrix – a diagonal matrix obtained by summing over rows. Throughout this work, this correction has proven to not affect the convergence of the results, whereas it presents an important computational advantage when it comes to solving a system with the matrix M.

5. Conclusions and final remarks

The present work introduces the nature and interpretation of Phase-Field models in the context of the Stefan problem, highlighting some of its advantages and limitations. One remarkable property, the approximation to the solution of the Stefan (sharp-interface) model for small ξ, is illustrated by a 2D analog of a 1D example with analytical solution. In addition, a further example with physical meaning is included.

Regarding the implementation, the code has been tested to be not only precise but also efficient, with a special mention to the use of the lumped mass matrix. Besides this, the limit $\xi \geq 1.25h$ has been seen to work in all cases.

An interesting extension of the work would be to surpass the assumptions made, by considering the generalized Stefan problem, as described in [4]. For example, different diffusivity constants c could be used for each phase (possibly with a linear approximation in the interface), or the latent heat could be modelled as a function of temperature $l(u)$. From a numerical perspective, the implementation of an adaptive mesh

– as done in [1] – would take full advantage of the FEM, while implicit time integration methods would allow larger time steps, but with the burden of having to solve a non-linear system of equations. The increased stability would allow the simulation of a wider class of phenomena, such as the coalescence of interfaces.

References

[1] G. Beckett, J.A. Mackenzie, M.L. Robertson, "A moving mesh finite element method for the solution of two-dimensional Stefan problems", *J. Comput. Phys.* **168(2)** (2001), 500–518.

[2] G. Caginalp, "An analysis of a phase field model of a free boundary", *Arch. Rational Mech. Anal.* **92(3)** (1986), 205–245.

[3] J.W. Cahn, J.E. Hilliard, "Free energy of a nonuniform system. I. Interfacial free energy", *J. Chem. Phys.* **28(2)** (1958), 258–267.

[4] J. Crank, *Free and Moving Boundary Problems*, Oxford Science Publications, The Clarendon Press, Oxford University Press, New York, 1984.

[5] M. Fabbri, V.R. Voller, "The phase-field method in the sharp-interface limit: A comparison between model potentials", *J. Comput. Phys.* **130(2)** (1997), 256–265.

[6] R. Kobayashi, "Modeling and numerical simulations of dendritic crystal growth", *Physica D: Nonlinear Phenomena* **63(3-4)** (1993), 410–423.

[7] L.D. Landau, E.M. Lifshitz, *Statistical Physics. Course of Theoretical Physics. Volume 5*, Third Edition, Part 1, Pergamon Press, London, 1980.

[8] J.T. Lin, "The numerical analysis of a phase field model in moving boundary problems", *SIAM J. Numer. Anal.* **25(6)** (1988), 1015–1031.

[9] A. Muixí, S. Fernández-Méndez, A. Rodríguez-Ferran, "Adaptive refinement for phase-field models of brittle fracture based on Nitsche's method", *Comput. Mech.* **66(1)** (2020), 69–85.

[10] A.C. Polycarpou, *Introduction to the Finite Element Method in Electromagnetics*, Synthesis Lectures on Computational Electromagnetics, Morgan & Claypool, 2006.

[11] N. Provatas, K. Elder, *Phase-Field Methods in Material Science and Engineering*, Wiley-VCH, 2010.

[12] J. Stefan, "Ueber die Theorie der Eisbildung, insbesondere über die Eisbildung im Polarmeere", *Ann. Phys.* **278(2)** (1891), 269–286.

[13] K.S. Surana, A.D. Joy, L.A. Quiros, J.N. Reddy, "Mathematical models and numerical solutions of liquid-solid and solid-liquid phase change", *Journal of Thermal Engineering* **1(2)** (2015), 61–98.

[14] A.A. Wheeler, W.J. Boettinger, G.B. McFadden, "Phase-field model for isothermal phase transitions in binary alloys", *Phys. Rev. A* **45(10)** (1992), 7424–7439.